Nucleic Acids Research, 2006, Vol. 34, No. 5 ***1381–1392***
doi:10.1093/nar/gkl008

Controlling RNA self-assembly to form filaments

Lorena Nasalean[1,2], Stéphanie Baudrey[3], Neocles B. Leontis[1,2] and Luc Jaeger[3,*]

[1]Department of Chemistry and [2]Center for Biomolecular Sciences, Bowling Green State University, OH 43402, USA and [3]Department of Chemistry and Biochemistry, Biomolecular Science and Engineering Program, Material Research Laboratory, University of California, Santa Barbara, CA 93106-9510, USA

Received as resubmission February 2, 2006; Revised and Accepted February 10, 2006

ABSTRACT

Fundamental control over supra-molecular self-assembly for organization of matter on the nano-scale is a major objective of nanoscience and nanotechnology. 'RNA tectonics' is the design of modular RNA units, called tectoRNAs, that can be programmed to self-assemble into novel nano- and meso-scopic architectures of desired size and shape. We report the three-dimensional design of tectoRNAs incorporating modular 4-way junction (4WJ) motifs, hairpin loops and their cognate loop–receptors to create extended, programmable interaction interfaces. Specific and directional RNA–RNA interactions at these interfaces enable conformational, topological and orientational control of tectoRNA self-assembly. The interacting motifs are precisely positioned within the helical arms of the 4WJ to program assembly from only one helical stacking conformation of the 4WJ. TectoRNAs programmed to assemble with *orientational compensation* produce micrometer-scale RNA filaments through supra-molecular equilibrium polymerization. As visualized by transmission electron microscopy, these RNA filaments resemble actin filaments from the protein world. This work emphasizes the potential of RNA as a scaffold for designing and engineering new controllable biomaterials mimicking modern cytoskeletal proteins.

INTRODUCTION

Biological systems rely almost exclusively on supra-molecular self-assembly to create complex supra-molecular structures that carry out diverse functions (1). Key characteristics of these systems are hierarchical organization, modular components and stereochemically specific interactions. The application of self-assembly principles gleaned from biological systems provides ways to achieve greater control over the design and construction of self-assembling molecular objects to produce artificial nano- and meso-scale devices to meet new chemical and biomedical challenges in the 21st century (2,3).

In the past 20 years, Seeman and co-workers explored nano-scale design principles using DNA. They have constructed geometrical objects on the nano-scale, including planar figures (4), regular polyhedrons (5,6) and knotted structures (7). More recently, they and others have used DNA double and triple cross-over junctions to construct rigid modular units (tiles) (8), programmed to self-assemble to generate two-dimensional (2D) patterned arrays (9,10) as well as various tubular structures (11–16). By introducing motifs that switch between alternative structures, DNA nanomechanical devices powered by 'fuel strands' have also been constructed (17). While these DNA structures have great potential for developing programmable, geometrically regular materials or templates for nanotechnology applications such as wiring nano-scale circuitry (11,13), the limitations of DNA as a biopolymer for mimicking biological functions carried out by proteins and RNA are also apparent.

While more chemically labile than DNA, natural RNAs comprise the working components of biologically important molecular machines, capable of using cellular energy in the form of ATP or GTP to perform mechanical work and to carry out complex tasks of information processing, such as template-directed protein synthesis (18–21) and multiplexed gene regulation (22–27). Natural RNAs are dynamic molecules that undergo large structural changes in carrying out specific functions. As such, they make use of a large variety of recurrent, modular and pre-organized structural motifs that mediate stereochemically precise and readily reversible, tertiary intra- and inter-molecular interactions (28,29). Analysis of the rapidly growing structural and sequence databases for RNA has revealed novel RNA–RNA interaction motifs and new topological rules for RNA three-dimensional (3D)

*To whom correspondence should be addressed. Tel: +1 805 893 3628; Fax: +1 805 893 4210; Email: jaeger@chem.ucsb.edu
Correspondence may also be addressed to Neocles B. Leontis. Tel: +1 419 372 8663; Fax: +1 419 372 9809; Email: leontis@bgnet.bgsu.edu
Present address:
Stéphanie Baudrey, Institut de Biologie Moléculaire et Cellulaire, 15 rue Descartes, F-67084 Strasbourg, France

assembly (29–34). 'RNA tectonics' refers to the application of the structural principles of modular design and hierarchical folding inferred from natural RNAs to create new nano- and meso-scopic self-assembling architectures (28,35,36). RNA is readily amenable to inverse folding: supra-molecular structures can be 'sketched' in 3D space by positioning modular motifs that mediate tertiary interactions to create the desired nano-scale architecture and then connecting the motifs using semi-rigid double helical 'struts'. Consequently, the design can be translated into an appropriate sequence designed to fold uniquely to form the desired structure (28,35–42). The positioning of structural elements can be controlled precisely, by adjusting the lengths of helices and their stacking arrangements at multi-helix junctions (28,35–37,39–41,43–45).

In previous works, we described the design of dimers (35,37,41,42), H-shaped (37) and square-shaped (36,45) modular RNA units, called tectoRNAs, that assemble into various nano-structures such as small RNA nanoparticles, one-dimensional (1D) and 2D arrays as well as addressable nano-grids of finite dimensions. Here, we present the first design and synthesis of RNA molecular units based on H-shaped molecules that self-assemble in a fully controllable manner to form oriented filaments. The self-assembly of these molecules is mediated by the positioning of specific hairpin loops and corresponding loop–receptors to create directional interfaces for non-covalent RNA–RNA interactions (35,37,41,42).

MATERIALS AND METHODS

Design and 3D modeling of H-shaped tectoRNAs

The sequence of each H-shaped tectoRNA was designed to avoid alternative secondary structure folds as previously described (35,36). Sequence designs were checked for proper folding by comparing the desired secondary structure with that predicted by mfold (www.bioinfo.rpi.edu/applications/mfold) (46). Atomic 3D models of H-shaped tectoRNAs were manually constructed '*in silico*' using MANIP (47) by connecting the 4-way junction (4WJ) extracted from the X-ray structure of the hairpin ribozyme (48) with two GAAA tetraloops and two 11 nt receptor modules extracted from the structure of the P4–P6 domain of the group I intron (49) using regular A-form RNA helices. Assembling interfaces were modeled according to previous 3D models of self-dimerizing tectoRNAs (35,37) to generate supra-molecular assemblies of molecules **1** and **2**. All the structural models were stereochemically refined with MANIP (47).

RNA preparation

All RNA molecules were prepared *in vitro* by T7 RNA polymerase run-off transcription of PCR generated templates as described previously (35,36) (see Supplementary Table A-1 for the complete list of synthetic DNA oligos used for making DNA templates for transcription). The migration of RNA on polyacrylamide gels (PAGE) was typically monitored by using ^{32}P-labeled RNA, either body labeled with [α-^{32}P]ATP or labeled at the 3′ end with [5′-^{32}P]pCp as described (35).

RNA self-assembly and native PAGE

RNA samples containing a fixed amount of body labeled RNA (2 nM) or RNA labeled on the 3′ end with [5′-^{32}P]pCp (0.1 nM) and sufficient unlabeled RNA to give the desired RNA concentrations were heated in water at 90°C for 1 min, immediately cooled on ice for 2 min and then allowed to assemble for 15–30 min at 30°C in 89 mM Tris-borate (pH 8.3), 15 mM or 30 mM $Mg(OAc)_2$, and 5% glycerol. For analysis, 10 µl of the RNA sample was combined with 1 µl of gel-loading buffer (same buffer with 0.01% bromophenol blue, 0.01% xylene cyanol) and run at 4°C typically on 7% (29:1) non-denaturing PAGE. The gel and running buffers were identical to those used for assembly except that glycerol was not included. Native gel electrophoresis was typically run for 3 h or overnight, with buffer recirculation, at ~4°C in the cold room. The gels were dried and autoradiographed using X-ray film or a phosphoimager screen. For K_d measurements, monomer and dimer bands were quantified on a phosphorimager and the dimer formation was correlated with RNA concentration. Equilibrium dissociation constants (K_d) were determined as the concentration at which half of the RNA molecules are dimerized (35).

Transmission electron microscopy

Unlabeled RNA samples for transmission electron microscopy (TEM) were prepared as described above in presence of 15 or 50 mM $Mg(OAc)_2$. A volume of 4 µl of self-assembled tectoRNA was placed on collodion-coated grids for 1 min. The sample was then washed in four sequential steps with solutions of 25, 50, 75% of ethanol in H_2O and 100% ethanol: each washing step consisted of 10 drops of wash solution dripped over the sample. The sample was then dried and tungsten-shadowed under high vacuum at 32 mA for 10 min and imaged at different nominal magnifications on a TEM (TEM JEOL100CX) at the Bowling Green State University EM Center. For comparison purposes, at least two samples were made with different [RNA] and/or [Mg^{2+}] for each molecule. These control grids underwent the same treatment as the regular samples.

RESULTS

H-shaped tectoRNA nomenclature

In previous work we introduced tectoRNA molecules designed to self-assemble at interfaces comprising pairs of RNA tertiary loop–receptor interactions (35,37). RNA hairpin loop/receptor interactions, while stereochemically precise and specific, are weak, and must be combined in pairs to be used for intermolecular association at low (sub-micromolar) concentrations. These H-shaped tectoRNAs comprise a 4WJ that organizes four interacting modules, GNRA tetraloops (L) or their cognate receptors (R), into two co-axially stacked domains (Helical Stacking domains: 'HS' domains).

Each tectoRNA can in principle interact with two other tectoRNAs through the formation of four loop–receptor interactions, two with each partner molecule. Due to the flexibility of the 4WJ motif, each molecule can adopt two different conformers, A and B (Figure 1A), which differ in the stacking arrangement of the helices at the 4WJ. For conformer

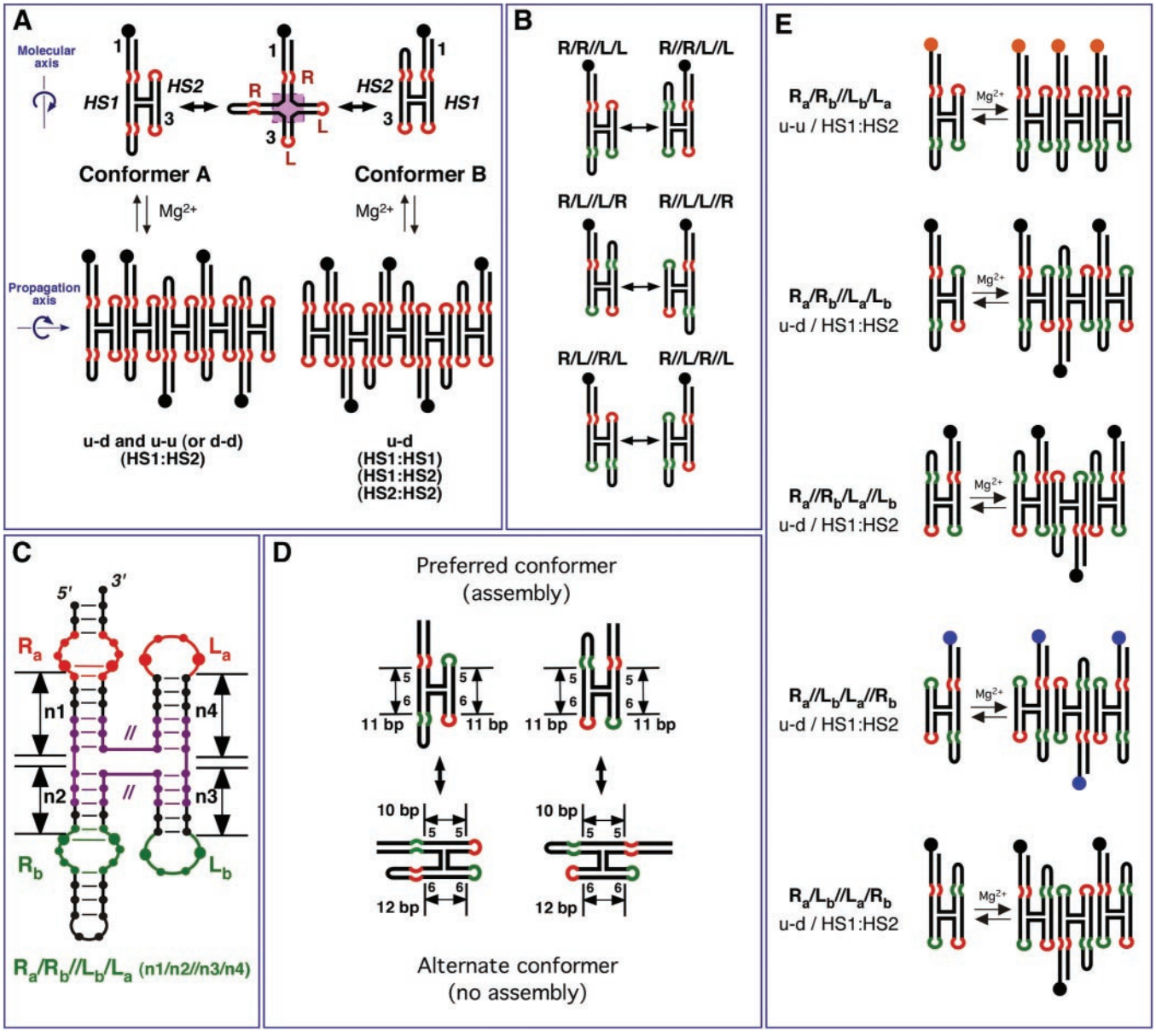

Figure 1. Assembly principles and nomenclature of H-shaped tectoRNA molecules based on hairpin tetraloops (L) and tetraloop receptors (R). (**A**) Scheme for self-assembly of H-shaped tectoRNA units into filaments. HS1 is defined as the stack that always contains stem 1, the one nearest to the 5′ end. HS2 is defined as the stack that always contains stem 3. Depending on the conformation (A or B), stems 2 and 4 can be in either stack HS1 or HS2. The 5′ end of the molecule, indicated by a solid circle, can be positioned upward ('u') or downward ('d') with respect to the axis of assembly propagation. Assembly can occur with 'up-up' ('u-u' or equivalently 'd-d') or 'up-down' ('u-d', i.e. alternating) orientation of two adjacent molecules with respect to the axis of propagation. (**B**) Schematic of all the possible strand topologies and conformers for H-shaped tectoRNAs comprising two loops and two receptors. (**C**) Nomenclature for H-shaped tectoRNA. Cognate loop/receptor motif pairs are indicated by the same color (red or green). The 4WJ motif is in magenta. (**D**) Structural principle for limiting efficient association of H-shaped tectoRNA to one conformer (A or B). Assembly is favored when the distance separating two stacked interaction modules in the same HS domain is 11 bp. (**E**) Directional self-assembly for H-shaped tectoRNAs with different strand topologies and conformations.

A, helical stack 1 (HS1) comprises helices 1 and 2 while helical stack 2 (HS2) comprises helices 3 and 4; for conformer B, HS1 comprises helices 1 and 4 and HS2 helices 2 and 3. Thus, HS1 is defined as the stacking domain that contains helix 1, defined as the helix with the 5′ and 3′ ends, and HS2 is defined to contain helix 3.

There are six ways of arranging the interacting modules for H-shaped tectoRNAs that each contains two loops and two receptors such that the first receptor is necessarily placed in the terminal stem 1 (Figure 1B). These correspond to three strand topologies, each of which generates two conformers by isomerization of the 4WJ. The following short hand notation will be used to designate the various topologies and conformations for each of the molecules described in this article. Starting from the 5′ end, each RNA module is listed as it appears sequentially. 'Ri' and 'Li' designate the interacting receptor and loop modules of type i, and the double forward slash, '//', indicates the 4WJ, where the strand crosses from one HS domain to the other (see Figure 1B). A single forward slash, '/', indicates helices belonging to the same HS domain

(see Figure 1B). We will designate the distances in base pairs separating each starred interacting module from the 4WJ by providing an additional annotation of the form n1/n2//n3/n4, where 'ni' indicates the distance in base pairs of the motif of helix i from the 4WJ, and '/' and '//' have the same meaning (Figures 1C and 2A). Thus, the complete annotation for describing molecule **9** in Figure 2 is Ra/Rb//Lb/La (5/6//5/6). Note that La is GAAA and Lb is GGAA.

Non-directional tectoRNA assembly

In the previous report (37), two different molecules were designed, each favoring one of the two 4WJ conformers, A or B (molecules **1** and **2** in Figure 2A). This was done by using the 4WJ motif of the hairpin ribozyme for which the sequence-dependent stacking preference is known (48,50). Molecule **1** favors conformer A and assembles with HS1 interacting exclusively with HS2 but randomly with respect to the axis of self-assembly propagation, in 'up-down' as well as 'up-up' (or 'down-down') fashion (Figure 1A). On the other hand, molecule **2** in conformer B is programmed to assemble in a strictly alternating 'up-down' fashion. However, random 180° rotation about the molecular axis perpendicular to the axis of propagation is possible, resulting in association through any combination of HS1 and HS2 in the interacting molecules (HS1:HS1, HS1:HS2 and HS2:HS2) (see Figure 1A). Thus, neither molecule **1** nor molecule **2** assemble with directional control.

As shown by native gel electrophoresis, molecule **1** multimerizes to form a range of products whereas molecule **2** only forms dimers [see (37) and Figure 4]. To better understand these differences in assembly, 3D atomic models of each molecule were generated and used to predict the outcome of oligomerization behavior for each possible combination of interfaces (Figure 3). Models show that molecules based on molecule **1** in conformation A that were designed to assemble directionally with 'up-down' alternation, should form left-handed supra-molecular filaments with a pitch of about eight molecules per supra-molecular turn (Figure 3B). 3D model building studies also show that 'up-up' (or 'down-down') assembly of molecule **1** leads to minor steric clashes if there is no change in the 4WJ conformations (data not shown). The interruption of sequential 'up-down' assembly by 'up-up' (or 'down-down') orientations of neighboring units generates kinks of the supra-molecular axis of ~45°. 3D model building studies on molecule **2** shows that of the three conceivable modes of self-assembly (i.e. HS1:HS1, HS1:HS2 and HS2:HS2) only HS1:HS2 can occur without producing serious steric clashes (Figure 3C). However, the dimers that result from HS1:HS2 interactions cannot grow further without producing major steric clashes. These clashes cannot be overcome by changing the conformation of the 4WJ.

In order to confirm our model building studies, we have now characterized these two tectoRNA assemblies by TEM and AFM (43). For molecule **1**, filaments no longer than 200 nm are observed by both techniques (for TEM, see Figure 5, top left). These are frequently interrupted by ~45° bends, corroborating the prediction. In addition, clusters of various sizes are observed (Figure 5, top left). In contrast, TEM for molecule **2** showed much smaller granular objects with size corresponding to dimers (Figure 5, top right).

Engineering directional tectoRNA assembly

Because molecules **1** and **2** assemble in a non-directional manner, they produce complex heterogeneous assembly products that are difficult to characterize. To obtain oriented 1D molecular arrays, two problems have to be overcome. First, it is necessary to limit assembly to one of the two possible conformers (A or B, Figure 1A). Second, each assembly interface has to be coded for unique and directional assembly.

TectoRNAs based on the 4WJ from the hairpin ribozyme favor one stacking conformation over the other by at most a few kcal/mol (50–52). For association to occur optimally, however, the distance between interacting motifs should be 11 bp—roughly the length of one RNA helical turn. For HS domains containing a GNRA loop in one helix and a loop–receptor in the other, this is the distance measured in bp between the GA trans Hoogsteen/Sugar-edge base pair in the GNRA hairpin loops and the GC Watson–Crick base pair within the receptors (both bps are marked by red stars for each tectoRNA design in Figure 2). For HS domains containing two loops or two receptors, this is the distance between the starred GA base pairs of the two loops or the starred GCs of the two receptors. Equilibrium dissociation constants (K_d) for different interfaces were measured using tectoRNAs designed with a single interface, so as to form dimers (Figure 2B). For interfaces with interacting GAAA loop/receptor motifs separated by the optimal distance 11 bp, the measured K_d was 4 nM (molecule **3**). When this distance was changed to 10 or 12 bp (molecules **3a** and **3b** in Figure 2B), the K_d increased from 4 to 80 or 110 nM, respectively (Figure 2C). No association was observed for a separation distance of 13 bp under similar conditions (molecule **3c** in Figure 2B). Therefore, to favor H-shaped tectoRNA association in one conformer (A or B) over association in the other, the positioning of the 4WJ must be adjusted so that the distance separating the interacting modules in each HS domain is exactly 11 bp only in the desired conformer (Figure 1D). Molecule **7** was derived from molecule **1** by moving HS2 one base pair down relative to the 4WJ (Figure 2A), so as to disfavor assembly from the alternate conformer B. Molecule **7**, like molecule **1**, assembles non-directionally and forms a variety of products (Figure 4A).

To create tectoRNA that assemble with directional control, an additional loop/loop–receptor pair was incorporated into the design. This makes it possible to create directional interfaces. The new interaction used in this work is the GGAA tetraloop (Lb) recognized by a receptor called C7.34 (Rb), previously selected by *in vitro* evolution (53) (Figure 2). In the monovalent dimer tectoRNA context, the K_d for the Rb/Lb homodimer is 40 nM (molecule **4**), 10 times higher than the Ra/La homodimer (molecule **3**) (Figure 2B). However, for the heterodimer resulting from Rb/La (molecule **5**) interacting with Ra/Lb (molecule **6**), the K_d is from 6 to 8 nM (41). This tectoRNA assembly is at least 20 times more selective for GGAA than any other GNRA loops, including GAAA. Indeed, molecules **5** and **6** self-dimerize with $K_d > 2$ μM and > 10 μM, respectively, as both homodimers require formation of two non-cognate interactions. The five basic constructs that were generated using two specific loop–receptor pairs are shown in Figure 1E with their modes of interaction: they all incorporate the design features described above and are expected to form polar and directional assemblies.

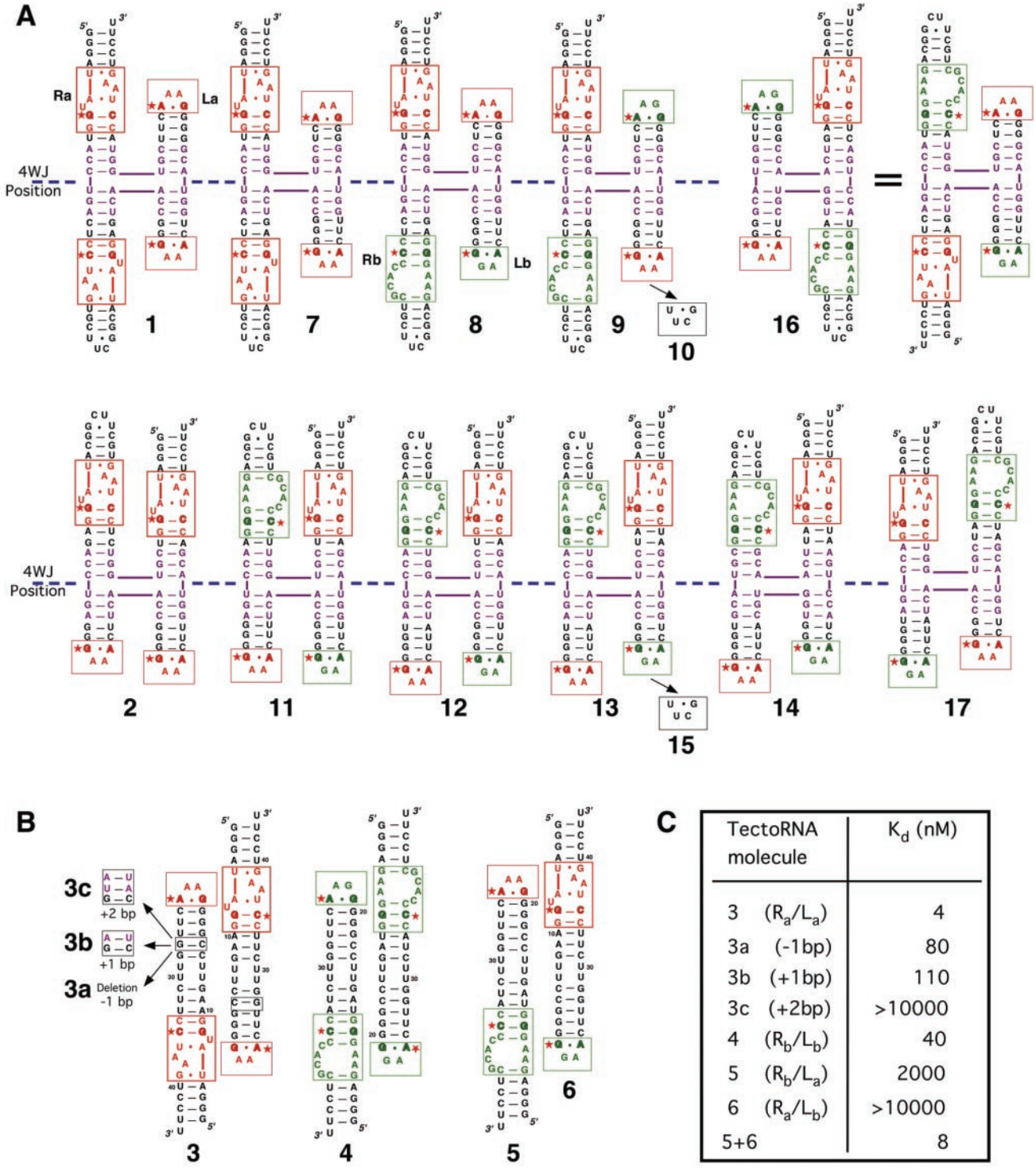

Figure 2. Secondary structure diagrams of tectoRNA molecules reported (see also Supplementary Table A-2). (**A**) H-shaped tectoRNAs: the positions of the conserved base pairs in the receptors and loops are shown in bold and indicated by a star; for optimal assembly, they are separated by 11 bp. Cognate loops and receptors are boxed and indicated by the same colors used in Figure 1D (red for La/Ra and green for Lb/Rb). Molecule **16** is shown in two different orientations, the one on the right conveys the structural similarities with molecule **9**. (**B**) Dimerizing tectoRNA molecules **3**, **4**, **5** and **6**, drawn to show their mode of interaction. Variants a, b and c of molecule **3** are indicated by arrows. (**C**) Table of equilibrium constants of dissociation (K_d) for dimerizing tectoRNAs displayed in (B). K_d were measured at 15 mM $Mg(OAc)_2$ as described previously (35,41).

Assembly of R/R//L/L tectoRNAs to form filaments

Two new molecules (**8** and **9**) were derived from molecule **7** by incorporating the second hairpin loop, GGAA ('Lb'), and its specific receptor, 'Rb' (Figure 2A). In molecule **8**, which is of type Ra/Rb//Lb/La, each hairpin and its cognate receptor are positioned on the same side of the 4WJ with respect to the axis of propagation of the assembly (Figure 1E). For molecule **9**,

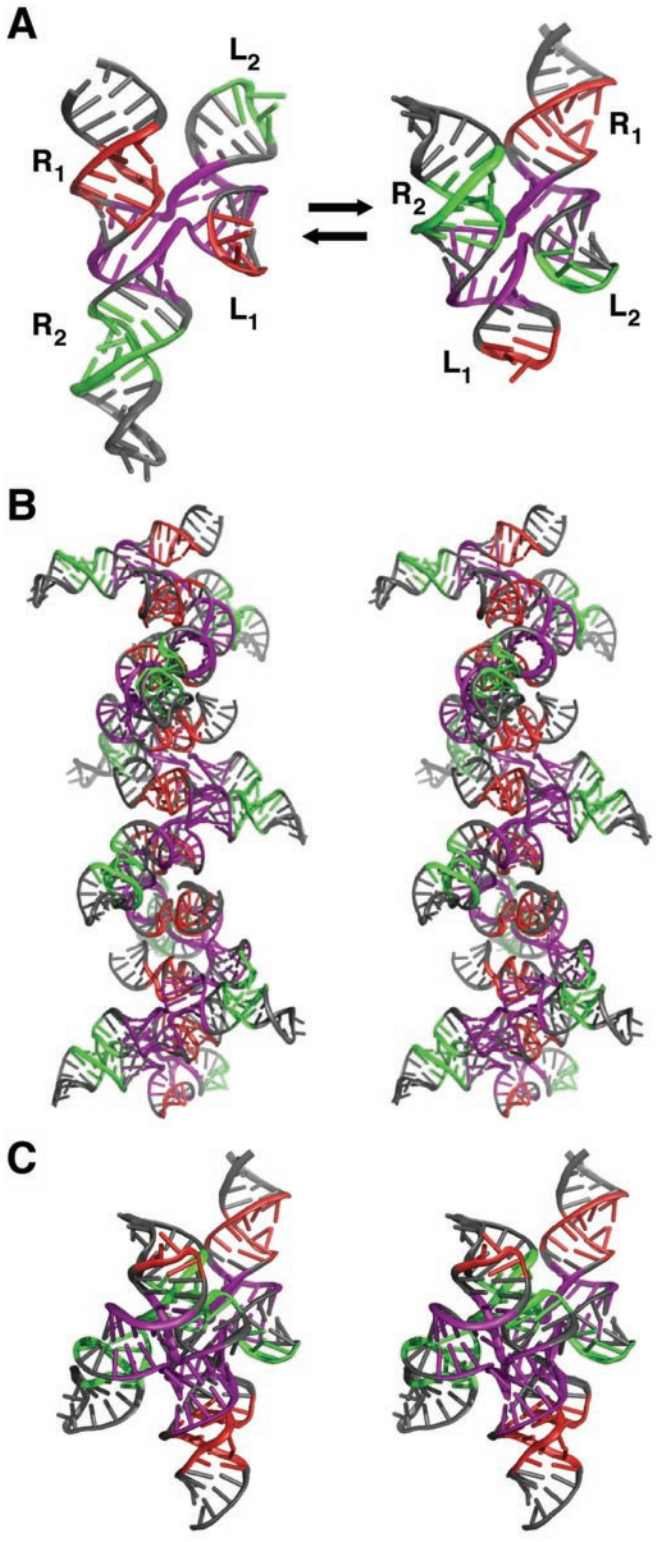

Figure 3. 3D models of H-shaped tectoRNAs **1** and **2**. (**A**) Molecules **1** (left) and **2** (right) correspond to two conformers that are in equilibrium. Stereoviews for molecule **1** filament (**B**) and molecule **2** dimer (**C**). These 3D models correspond to assemblies [u-d (HS1:HS2)] that maintain the structure of the 4WJ (in violet) as observed in the hairpin ribozyme X-ray structure without producing any inter-molecular steric clashes. In these models, HS1 (containing R1) of 1 U interacts with HS2 (containing L1) of another unit so that the interacting motifs R1–L1 (in red) and R2–L2 (in green) can associate.

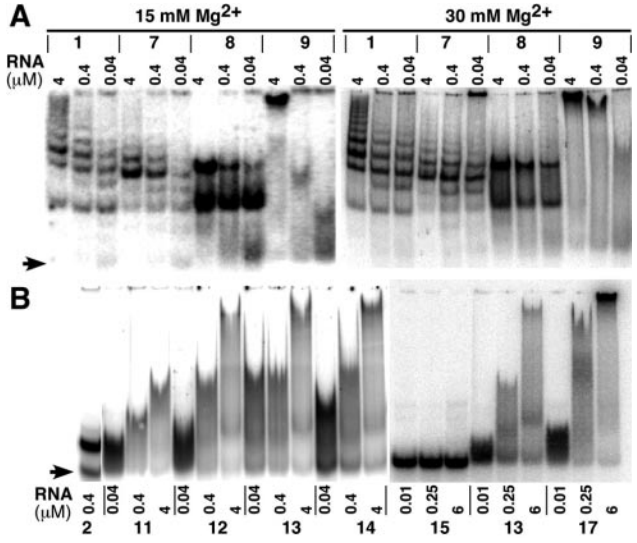

Figure 4. Supra-molecular assembly of various 4WJ tectoRNA visualized on native PAGE. (**A**) Self-assembly of molecules **1**, **7**, **8** and **9** at 15 and 30 mM of Mg^{2+}. (**B**) Self-assembly of molecules **2**, **11**, **12**, **13**, **14**, **15** and **17** at 15 mM Mg^{2+}. Experiments were carried out in the presence of 15 or 30 mM $Mg(OAc)_2$ as described in the Materials and Methods. Arrows indicate the expected positions of monomer bands.

which is of type Ra/Rb//La/Lb, the positions of the loops, La and Lb, are switched compared to molecule **8** (Figure 1E). Thus, molecule **8** assembles directionally with each successive monomer in the same ('up') orientation, while molecule **9** assembles directionally with 'up-down' alternation. Interestingly, molecule **9** assembles in a highly concentration-dependent manner to form long fibers at μM RNA concentrations that are very sensitive to [Mg^{2+}] (Figure 4A). Molecule **8**, on the other hand, assembles into specific oligomeric complexes even at low Mg^{2+} and sub-nanomolar RNA concentrations (Figure 4A). We have determined that the smallest complex formed by molecule **8** is a trimer (B. Hassan, M. Mirzoyan, K. Afonin, L. Nasalean, L. Jaeger and N. Leontis manuscript in preparation). A larger complex of molecule **8** forms at micromolar RNA concentrations and is favored by higher [Mg^{2+}] and appears by gel electrophoresis to consist of 5–7 U (Figure 4A). The formation of a closed complex is corroborated by TEM studies of molecule **8**, which show toroidal structures of uniform size, ~6 nm in diameter, and thus larger than the dimer complexes of molecule **2** (Figure 5, middle right). The formation of closed trimer complexes is also corroborated by 3D modeling: closed trimer complexes can form easily by adjustment of the angle of the 4WJ to allow the HS domains, HS1 and HS2, in each tectoRNA unit to achieve a nearly parallel configuration. This conformational change makes it possible for each pair of tectoRNAs in the trimer to form two cooperative loop–receptor interactions (B. Hassan, M. Mirzoyan, K. Afonin, L. Nasalean, L. Jaeger and N. Leontis manuscript in preparation).

TEM characterization shows that molecule **9**, in contrast with molecule **8**, forms filaments that are up to 1 μm in length, much straighter than those formed by molecule **1** and tend to align side-by-side to form loose sheets (Figure 5, middle and bottom left). Molecule **9** was designed to assemble uniformly and directionally with 'up-down' alternation, whereas

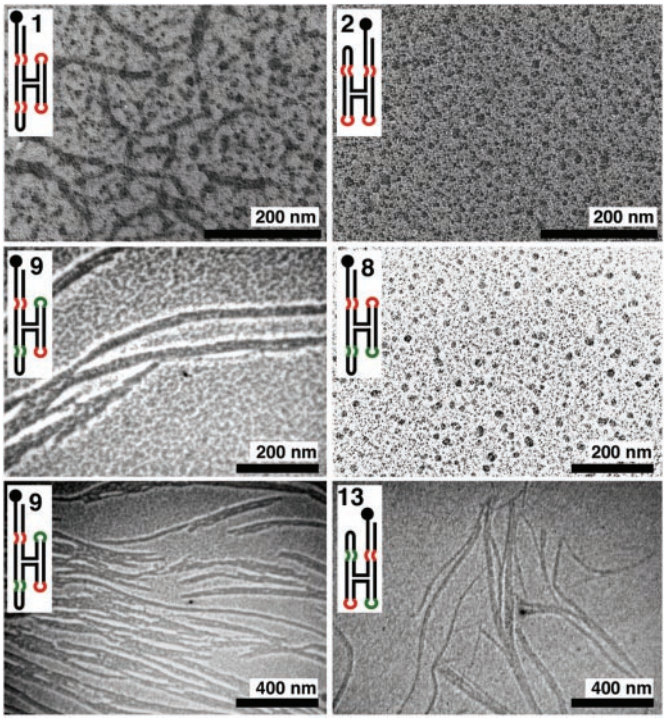

Figure 5. Visualization of RNA supra-molecular assembly by TEM. Molecules **1** (top left) and **2** (top right): RNA samples were prepared with 15 mM Mg^{2+} as described in the Materials and Methods; molecule **9** (middle and bottom left), molecule **8** (middle right) and molecule **13** (bottom right): RNA samples were prepared with 50 mM Mg^{2+} as described in the Materials and Methods. Background speckles are due to grains of tungsten.

molecule **1** monomers can be added to the ends of filaments with 'up-up' or 'up-down' orientation. The discrete RNA bands observed by gel for assembly of molecules **1** and **7** are thus probably due to random insertion of monomers with 'up-up' orientation which results in steric clashes that limit the further growth of the filaments, consistent with 3D modeling discussed above.

Other molecules were derived from molecules **8** and **9** by changing the positioning of the 4WJ relative to the interacting motifs (see Supplementary Table A-2) and found to assemble into clusters or filaments. However, none of these molecules formed filaments as long or as straight as the parent molecule **9** at 15 mM Mg^{2+} (see Supplementary Table A-2). Substitution of one of the GAAA tetraloops of molecule **9** by a terminating loop (UUCG tetraloop) completely prevented association (molecule **10** in Figure 2A), indicating that two intact specific loop–receptor interactions are needed for assembly at micromolar or lower concentrations. UNCG loops have very different tertiary structures and do not bind to GNRA receptors.

Assembly of R//R/L//L tectoRNAs to form filaments

Based on our experience with molecules **8** and **9**, it became apparent that molecule **2**, Ra//Ra/La//La (5//6/5//6), could also be engineered to form filaments because of the 'up-down' alternation that occurs when the R//R/L//L conformer assembles. According to 3D modeling, assembly of R//R/L//L molecules could be promoted by changing the position of the 4WJ relative to the interacting motifs so as to avoid steric clashes while also preventing assembly from the alternate conformer, and by introducing a second loop–receptor motif to prevent interface promiscuity. We created a series of molecules in which the HS2 domain was moved 1 bp at a time relative to the HS1 domain at the 4WJ. The first molecule in this series, molecule **11**, Ra//Rb/La//Lb (5//5/6//6), was derived from molecule **2** by moving HS2 down 1 bp to disfavor assembly from the alternate conformer and by introducing the second specific loop/receptor pair, Lb/Rb, to prevent HS1:HS1 or HS2:HS2 association (Figures 1E and 2A). Thus, molecule **11** only assembles with alternating 'up-down' orientation through interaction of HS1:HS2 interfaces. This results in directional assembly similar to molecule **9** and, not unexpectedly, molecule **11** also forms concentration-dependent multimers (equilibrium polymers) on native gels. At low concentration, molecule **11** forms dimers, but as the RNA concentration increases equilibrium polymers are observed (Figure 4B). Interestingly, the next molecule in the series, molecule **12**, Ra//Rb/La//Lb (5//4/7//6), forms longer multimers, more closely resembling those of molecule **9** of the R/R//L/L series (Figure 4B). Only slight further improvements in the length of filaments were observed for molecules **13** and **14** (Figure 4B), which were derived from **12** by moving HS1 one base pair up with respect to HS2 at the 4WJ, giving the geometry Ra//Rb/La//Lb (6//4/7//5) (see Figure 2A). As shown by TEM (Figure 5, bottom right), molecule **13**, like molecule **9**, forms long and regular filaments that also show a tendency to align with each other. Molecules **13** and **14** differ by a 180° rotation of the local sequence of the 4WJ motif relative to the helical arms (see Figure 2A and Supplementary Table A-2). This change maintains the same stacking geometry in molecules **13** and **14**. As both molecules behave similarly, this suggests that the structure of the 4WJ has a 2-fold rotational pseudo-symmetry (C2). Similar results were obtained for 4WJ variants of molecules **8** and **9** (molecules **8c** and **9d**—see Supplementary Table A-2). As for R/R//L/L tectoRNAs, assembly of R//R/L//L variants requires two intact loop–receptor interactions at each interaction interface. Substitution of one interacting tetraloop of molecule **13** by a non-interacting UUCG loop (molecule **15** in Figure 2A) abolished the association.

Assembly of R//L/L//R and R/L//L/R tectoRNAs to form filaments

We drew on our new understanding of the rules and modes of self-assembly of molecules belonging to the R/R//L/L and R//R/L//L series to design additional tectoRNA molecules with R//L/L//R and R/L//L/R strand topologies, also capable of forming extended filaments. Despite different strand topology, molecule **16**, Ra//Lb/La//Rb (6//6/5//5) is structurally equivalent to molecule **9**, Ra/Rb//La/Lb (5/6//6/5) with helical stems 1, 2, 3 and 4 of molecule **16** corresponding to helical stems 2, 3, 4 and 1 of molecule **9** (Figures 1E and 2A). Thus, the conserved GC Watson–Crick base pair of the receptors and the GA Hoogsteen/Sugar-edge base pair of the GNRA tetraloops of **16** are superimposed with those of **9**, positioning these interacting elements at the same distance from the 4WJ. In the same way, molecules **13** and **17** are structurally equivalent, with helical stems 1, 2, 3 and 4 of molecule **13** corresponding to helical stems 4, 1, 2 and 3 of molecule **17** (Figures 1E and 2A). The receptors, Ra and Rb, as well as the loops, La and Lb,

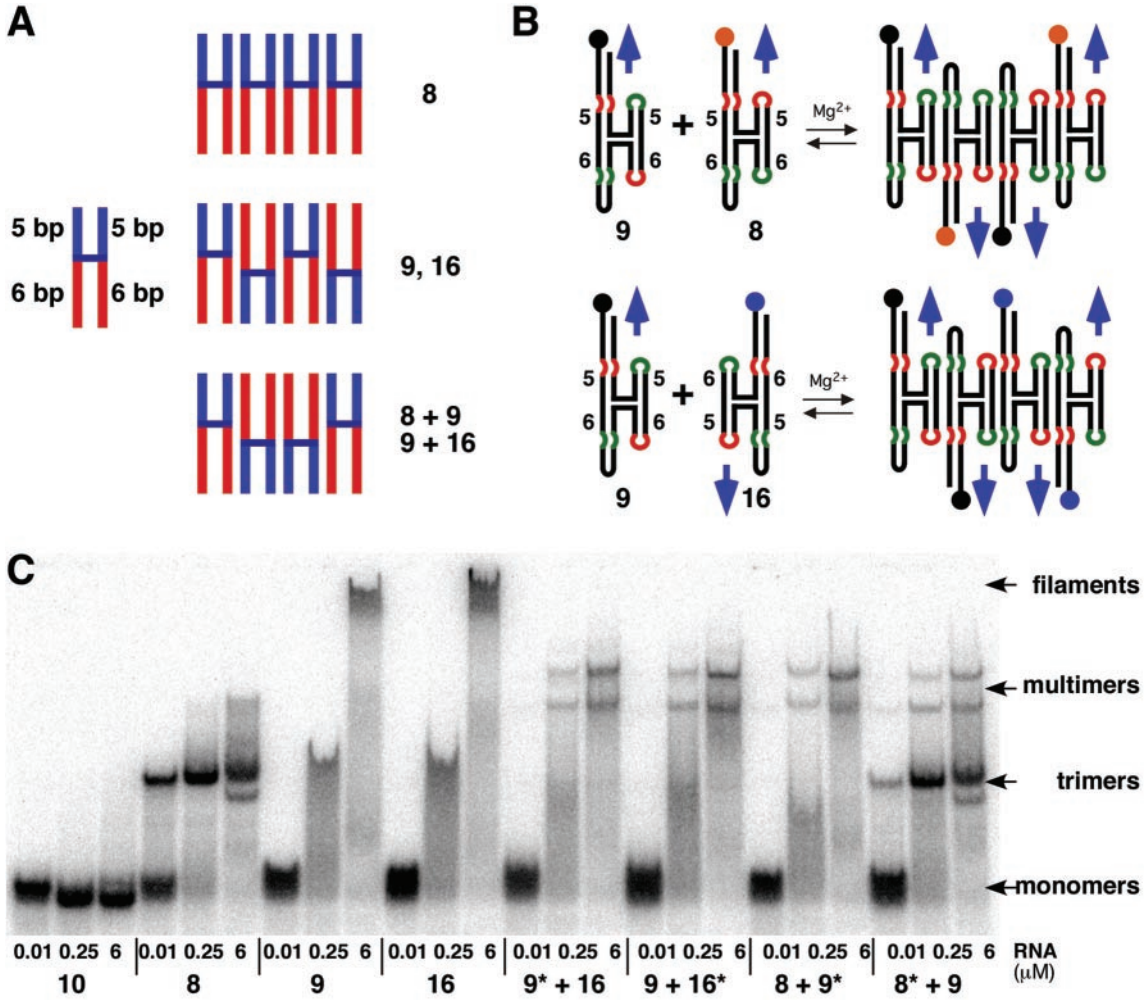

Figure 6. The principle of orientational compensation. (**A**) Schematic representation of molecules **8**, **9** and **16** to highlight asymmetry in the length of the helical arms and modes of interaction: The blue color indicates the helical arms in which the distance separating the interacting motifs from the 4WJ is 5 bp and the red color indicates the helical arms for which this distance is 6 bp. Molecule **8** self-assembles 'up-up,' molecules **9** and **16** self-assemble 'up-down,' and mixtures of molecules **9** and **8** or **9** and **16** self-assemble with both 'up-up' and 'up-down' associations. (**B**) Detailed schematic of 'up-up' and 'up-down' interactions in the assembly of molecule **9** with **8** (upper panel) and **9** with **16** (lower panel). (**C**) Supra-molecular assembly of mixtures of molecule **9** with molecule **8** or **16** visualized on native PAGE with self-assembly of **10** (monomer), **8**, **9** and **16** shown as controls. The radiolabeled RNA molecule is indicated by an asterisk (*) and is present in 0.1 nM concentration. The samples were prepared in presence of 15 mM $Mg(OAc)_2$ and visualized on 7% (1:30) native PAGE as indicated in the Materials and Methods.

are swapped in molecule **16** relative to their positions in molecule **9**, and likewise for **17** vis-à-vis **13**.

Molecules **16** and **17**, like **9** and **13**, are asymmetric as regards the distances of the interacting motifs from the 4WJ. For molecules **9** and **16**, the distance is 5 bp for helices on one side of the 4WJ, shown in blue in Figure 6A, and 6 bp for helices on the other side of the 4WJ, shown in red. One must pay attention to this asymmetry to define, in a consistent manner, the relative orientations of molecules when they assemble. We arbitrarily designate as 'up' the 'blue' side of molecules **8**, **9** and **16**, i.e. the side in which the interacting motifs are positioned 5 bp from the 4WJ. To highlight its structural equivalence to molecule **9**, the secondary structure of molecule **16** is also shown rotated 180° in Figure 2A, with helix 1 (containing the 5′ and 3′ ends) pointing downward and helices 2 and 3, which have motifs positioned 5 bp from the 4WJ, oriented upward. This orients the 'blue' helices of **16** toward the top of the page consistent with Figure 6A. For molecules **13** and **17**, the helices that have the receptors positioned 4 and 6 bp from the 4WJ are assigned the 'up' orientation.

Because molecules **16** and **17** are structurally equivalent to **9** and **13**, respectively, they also assemble with 'up-down' alternation and, as shown by native PAGE, both form very long filaments when assembled at μM RNA concentrations in the presence of 15 mM magnesium ions, as predicted (see Figure 6C for molecule **16** and Figure 4B for molecule **17**). This experiment corroborates the determining role of 'up-down' alternation in the assembly of H-shaped tectoRNA to form extended filaments.

Assembly with mixtures of H-shaped tectoRNAs

To explore the generality of these ideas concerning the role of orientational compensation, we examined the behavior of mixtures of tectoRNA molecules. When molecule **8** is mixed with **9**, both 'up-up' and 'up-down' associations are expected to occur, as shown in Figure 6B, in which bold blue arrows are

used to indicate the 'up' orientation of each molecule as it assembles. Thus, HS2 of molecule **8** should associate with HS1 of molecule **9** in 'up-up' (or 'down-down') fashion, while HS2 of molecule **9** should associate with HS1 of molecule **8** with 'up-down' alternation (see also Figure 6A). Based on these considerations, we expected mixtures of **8** and **9** to form blocked or possibly closed complexes, rather than filaments such as those molecule **9** forms alone. Furthermore, we expected complexes formed by **8** and **9** to be larger than those formed by **8** alone. Native PAGE shows that indeed equimolar mixtures of molecules **8** and **9** form discrete complexes that are larger than the trimers formed by **8** alone (Figure 6C). Use of radiolabeled molecules **8** and **9** in separate experiments demonstrates that both molecules are present in these larger complexes (Figure 6C). Using radiolabeled molecule **8**, one sees that, at sufficiently high concentrations of molecule **9**, the cooperative trimer complexes of molecule **8** are disrupted in favor of the larger complexes that incorporate molecule **9**.

Similar considerations indicated that mixing molecules **9** and **16** should also produce discrete complexes, even though in this case both **9** and **16** individually produce long filaments. Indeed, HS2 of **9** should associate with HS1 of **16** in uncompensated 'up-up' fashion. Likewise, HS2 of **16** and HS1 of **9** should associate 'up-up'. As for molecules **8** and **9**, 'up-up' for molecules **9** and **16** means that the molecules associate so that their interacting motifs are positioned the same distance from the 4WJ. Thus, mixtures of **9** and **16** should produce the same results as **9** and **8**, and indeed mixtures of **9** and **16** also produce discrete complexes having identical gel mobilities as those produced by mixtures of **9** and **8** (Figure 6C).

The 'up-up' (or 'down-down') associations that result when **9** and **16** interact, disrupt the strict 'up-down' alternation that produces the filaments formed when either **9** or **16** assemble alone. The 'up-up' interactions in the **9** + **16** mixtures introduce a curvature in the filaments that shorten their lengths and may even allow closed complexes to form, as occurs for molecule **8**. Figure 6B shows that identical patterns of 'up-up' and 'up-down' assembly are possible when **9** is mixed with either **8** or **16**. This diagram presents, for illustrative purposes only, one possible sequence of assembly that molecule **9** can form with both molecule **8** and molecule **16**, to account for the fact that both mixtures form discrete complexes with identical gel mobilities. The exact order in which these molecules assemble to form the discrete complexes observed in the gels is the subject of future work (Figure 6C).

DISCUSSION

In previous studies (37,43), we showed that H-shaped tectoRNA molecules can form supra-molecular 1D assemblies using lateral tertiary interactions. However, these assemblies were not homogeneous. In this article we have shown how to modify the original H-shaped tectoRNA designs to create programmable, polar and directional 1D arrays.

In polar tectoRNA arrays, the HS1 domain of each tectoRNA associates only with the HS2 domain of the preceding tectoRNA. In directional arrays, the tectoRNA units are programmed to associate exclusively 'up-up' or 'up-down' at the interaction interfaces. If the interacting interfaces of HS1 and HS2 were related by an exact pseudo-dyad symmetry of 180° with respect to the perpendicular molecular axis, the resulting linear assemblies would be straight regardless whether the molecular units assemble with 'up-up' or 'up-down' orientation [Figure 7A and C, case (a)]. Recently, artificial three-helix and six-helix bundle DNA tiles were reported that belong to this category and assemble into programmable linear arrays (13,14).

As H-shaped tectoRNA molecules are fully asymmetric structures with interaction interfaces that are not oriented exactly 180° to each other, assemblies of molecules designed to associate with 'up-up' orientation generate a curvature that is not locally compensated along the axis of propagation of the

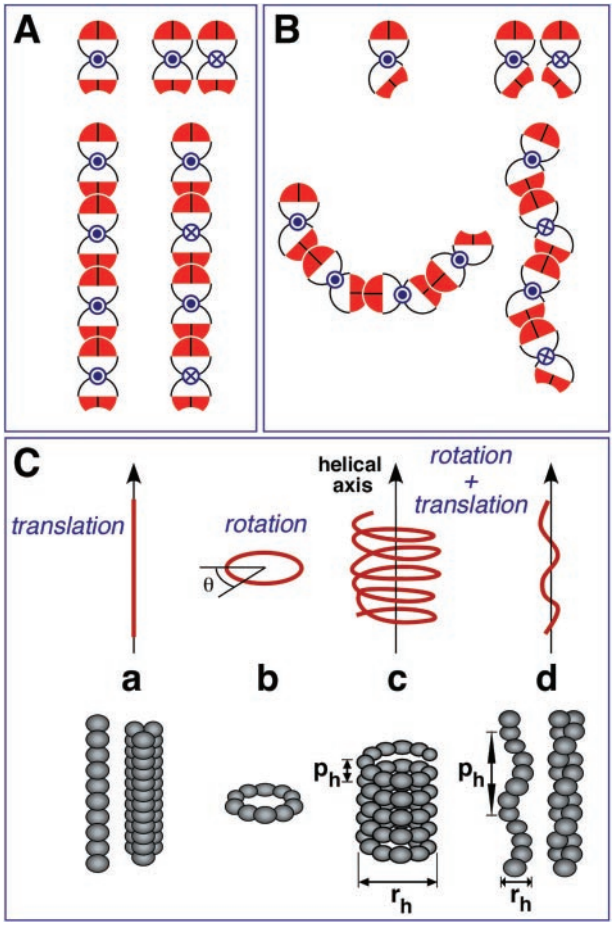

Figure 7. Modes of assembly of tectoRNA molecules comprising two HS domains (shown as connected circles) and having complementary interaction interfaces (shown in red). The up versus down orientations are distinguished by the blue circle or dot at the position of the 4WJ, connecting the two HS domains. (**A**) In the hypothetical case of perfectly opposed interacting interfaces, straight filaments are produced by either 'up-up' (left) or alternating 'up-down' (right) self-assembly. (**B**) In the actual case that the interfaces are not perfectly opposed, 'up-up' assembly produces curvature (left) while alternating up-down assembly compensates the asymmetry at the interfaces (right). Note that changing the angle between interfaces affects the radius of curvature in 'up-up' assembles while 'up-down' assemblies remain straight. (**C**) Hypothetical filaments produced by simple translation (**a**) of units with perfectly opposed interfaces. (**b**) Closed complexes produced by 'up-up' assembly confined to a single plane. (**c**) Helices with large helical radius (r_h) and short helical pitch (p_h) produced by 'up-up' assembly. (**d**) Extended helices with small radius and long pitch produced by 'up-down' alternation. Association of parallel filaments to form bundles or intertwined helices is also shown for cases (a) and (d).

resulting filament (Figure 7B). Evidently, for molecule **8**, the assembly is confined to a plane so that closed, cooperative complexes form (Figure 7B). In contrast, tectoRNAs that were programmed to associate exclusively with 'up-down' alternation consistently formed microfilaments at sufficiently high RNA concentrations, as long as steric clashes were avoided at successive interfaces. In this case, local compensation occurs in the orientation of the chiral tectoRNA units with respect to the axis of propagation of the filament, and straight filaments can form as observed for molecule **9** (Figure 7B). Thus, introduction of 180° orientational compensation at the interaction interface appears to eliminate one source of asymmetry (Figure 7B), favoring the production of μm-long filaments with left-handed supra-molecular helical shapes, according to modeling studies (Figure 3B and L. Jaeger and N. Leontis, unpublished results).

In 1950, Crane (54) identified a fundamental principle of self-assembly—that helices are the simplest infinite linear arrays of repeating units, as they result from the application of a general rotatory-translation operation. Drawing on Crane's work, Linus Pauling in 1953 (55) considered the types of structures that can form when protein molecules self-assemble using two complementary binding sites (surfaces). He noted that if the pitch of the helix (p_h) is less than the width of the molecule in the direction of the axis of the helix, steric hindrance prevents formation of a filament and finite, 'blocked,' asymmetric oligomers form. When the pitch of the helix is nearly zero and the rotational operation that transforms each subunit into its neighbor is nearly 360° divided by an integer, *n*, the combined flexibility in the intermolecular interactions and in the internal conformation of the subunits may produce closed complexes in the form of a ring, with *n* subunits and *n* inter-subunit bonds [shown schematically for the general case (b) in Figure 7C]. Such complexes have an n-fold symmetry axis. This is the case for molecule **8**, which forms a closed trimer complex (B. Hassan, M. Mirzoyan, K. Afonin, L. Nasalean, L. Jaeger and N. Leontis, manuscript in preparation).

When the pitch of the helix is approximately equal to the thickness of the molecule in the direction of the axis of the helix and the molecules in successive turns of the helix can bond with each other, a fibril stabilized by longitudinal associations may result. Tubular, possibly hollow, structures form, depending on the number of subunits per turn and their diameters relative to that of the helix [Figure 7C, case (c)]. If the pitch of the helix is approximately equal to an integral multiple of the diameter of a molecule in the direction of the axis of the helix, a tubular fibril involving two or more interpenetrating helices may form. Most natural linear assemblies of proteins, including microtubules and bacterial flagella, are tubular in structure (56–58). Interestingly, artificial programmable DNA nanotubes belonging to this category were recently reported that form as a consequence of bending within their component double or triple cross-over tiles (11,12,16). However, their shapes are not fully controllable, as they assemble to form hollow nanotubes of variable circumferences (12).

Tighter, narrower filaments, without a central hollow can be built by orienting the binding surfaces so that only a small number of subunits compose each turn [Figure 7C, case (d)] (59). The filaments produced by tectoRNA molecules **9**, **13**, **16** and **17** belong to this category, as do thin filaments, which are principally composed of actin (60,61), intermediate filaments (62) and most, if not all, reported artificial linear assemblies of engineered peptide and proteins (56,63,64). Like intermediate filaments, most of these engineered filaments are not polar and the individual filaments generally aggregate to form bundles ranging from 50 to 100 nm in diameter (56). In contrast, tectoRNA filaments with 'up-down' alternation are polar and directional like actin assemblies. The intrinsic twist of the 4WJ of each subunit produces left-handed supra-molecular helices with a small radius and long pitch, with up to 8 U per helical turn. F-actin forms a left-handed supra-molecular helix with 13 actin molecules per 6 helical turns. The rotation per molecule along the filament axis is close to 166° (almost 180°). The pitch of the actin helix is one molecular diameter and each molecule interacts longitudinally with the molecules in neighboring helical turns. In fact, these longitudinal interactions appear to be more extensive than the lateral interactions that produce the generic helix (61). Thus, the actin helix appears morphologically as two right-handed, steep helices that twine slowly round each other [see Figure 7C, case (d)].

CONCLUSION

The modular structure and hierarchical assembly properties of RNA make it very amenable to rational design for nano- and meso-scopic construction using supra-molecular assembly (28,35,36). Different tertiary interaction motifs with different specificities can exhibit very similar interaction geometries and therefore can be modularly swapped to redirect supra-molecular assembly (28) (C. Geary, S. Baudrey, N. Leontis and L. Jaeger manuscript in preparation). This property of RNA is exploited in the present work to precisely control the orientation of assembly between consecutive tectoRNA units along and perpendicular to the axis of assembly. By combining three or more distinct swappable interacting motifs, programmable assembly of a population of tectoRNA molecules, each differing in the positioning of specific loops and receptors, can thus be achieved to produce even more complex supra-molecular RNA architectures. The central role of RNA in complex biological machineries such as the ribosome (18–21), the DNA packaging motor of phage Phi29 (65) or bacterial riboswitches (22) suggests that complex dynamical functions can be engineered using RNA. Future work will explore the possibilities of exploiting RNA to engineer filaments with potential functions similar to those of modern cytoskeletal proteins.

The central involvement of RNA in modern living organisms suggests that it is not a fossil but a modern molecule with unique intrinsic properties not fully substituted by DNA or protein. In the future, RNA will likely play a major role in the development of new responsive biomaterials with potential applications in nanotechnology, biotechnology and medicine (36,44,66–68).

SUPPLEMENTARY DATA

Supplementary Data are available at NAR Online.

ACKNOWLEDGEMENTS

This work is dedicated to Saint Albert the Great, patron saint of scientists. L.J. and N.B.L. wish to thank Eric Westhof for his support in the early stage of this work, when L.J. was still working at the IBMC, Strasbourg, France. Funding for this work was provided by grants from the National Institutes of Health (2 R15 GM055898-03 to NBL), the American Chemical Society (ACS PRF# 42357-AC 4 to N.B.L.) and the National Science Foundation (CHE-0317154 to L.J.), and a grant subcontract from the University of Glasgow (MINT) to L.J. In 2002, initial experiments were also partially funded by EU project IST-2001-32152 (MINT). The authors acknowledge the assistance of Prof. Carol Heckman, Dan Schwab and Marilyn Cayer of the BGSU Electron Microscopy Center. We thank Brian Yard and Randy Like for technical assistance, Erik Verzemnieks for making Figure 3 and Arkadiusz Chworos, Cody Geary and Martin Sagermann for critical reading of the manuscript. Funding to pay the Open Access publication charges for this article was provided by NSF.

Conflict of interest statement. None declared.

REFERENCES

1. Goodsell,D.S. (2004) *Bionanotechnology: Lessons from Nature*. Wiley-Liss, Hoboken, New Jersey.
2. Whitesides,G.M. and Boncheva,M. (2002) Beyond molecules: self-assembly of mesoscopic and macroscopic components. *Proc. Natl Acad. Sci. USA*, **99**, 4769–4774.
3. Roco,M.C. (2003) Nanotechnology: convergence with modern biology and medicine. *Curr. Opin. Biotechnol*., **14**, 337–346.
4. Seeman,N.C. (1998) DNA nanotechnology: novel DNA constructions. *Annu. Rev. Biophys. Biomol. Struct*., **27**, 225–248.
5. Zhang,Y. and Seeman,N.C. (1994) The construction of a DNA octahedron. *J. Am. Chem. Soc*., **116**, 1661–1669.
6. Shih,W.M., Quispe,J.D. and Joyce,G.F. (2004) A 1.7-kilobase single-stranded DNA that folds into a nanoscale octahedron. *Nature*, **427**, 618–621.
7. Du,S.M., Wang,H., Tse-Dinh,Y.C. and Seeman,N.C. (1995) Topological transformations of synthetic DNA knots. *Biochemistry*, **34**, 673–682.
8. Seeman,N.C. (2005) Structural DNA nanotechnology: an overview. *Methods Mol. Biol*., **303**, 143–166.
9. Winfree,E., Liu,F., Wenzler,L.A. and Seeman,N.C. (1998) Design and self-assembly of two-dimensional DNA crystals. *Nature*, **394**, 539–544.
10. Yan,H., LaBean,T.H., Feng,L. and Reif,J.H. (2003) Directed nucleation assembly of DNA tile complexes for barcode-patterned lattices. *Proc. Natl Acad. Sci. USA*, **100**, 8103–8108.
11. Liu,D., Park,S.H., Reif,J.H. and LaBean,T.H. (2004) DNA nanotubes self-assembled from triple-crossover tiles as templates for conductive nanowires. *Proc. Natl Acad. Sci. USA*, **101**, 717–722.
12. Rothemund,P.W., Ekani-Nkodo,A., Papadakis,N., Kumar,A., Fygenson,D.K. and Winfree,E. (2004) Design and characterization of programmable DNA nanotubes. *J. Am. Chem. Soc*., **126**, 16344–16352.
13. Park,S.H., Barish,R., Li,H., Reif,J.H., Finkelstein,G., Yan,H. and Labean,T.H. (2005) Three-helix bundle DNA tiles self-assemble into 2D lattice or 1D templates for silver nanowires. *Nano Lett*., **5**, 693–696.
14. Mathieu,F., Liao,S., Kopatsch,J., Wang,T., Mao,C. and Seeman,N.C. (2005) Six-helix bundles designed from DNA. *Nano Lett*., **5**, 661–665.
15. Endo,M., Seeman,N.C. and Majima,T. (2005) DNA tube structures controlled by a four-way-branched DNA connector. *Angew. Chem. Int. Ed. Engl*., **44**, 6074–6077.
16. Mitchell,J.C., Harris,J.R., Malo,J., Bath,J. and Turberfield,A.J. (2004) Self-assembly of chiral DNA nanotubes. *J. Am. Chem. Soc*., **126**, 16342–16343.
17. Seeman,N.C. (2005) From genes to machines: DNA nanomechanical devices. *Trends Biochem. Sci*., **30**, 119–125.
18. Noller,H.F., Hoang,L. and Fredrick,K. (2005) The 30S ribosomal P site: a function of 16S rRNA. *FEBS Lett*., **579**, 855–858.
19. Frank,J., Sengupta,J., Gao,H., Li,W., Valle,M., Zavialov,A. and Ehrenberg,M. (2005) The role of tRNA as a molecular spring in decoding, accommodation, and peptidyl transfer. *FEBS Lett*., **579**, 959–962.
20. Baram,D. and Yonath,A. (2005) From peptide-bond formation to cotranslational folding: dynamic, regulatory and evolutionary aspects. *FEBS Lett*., **579**, 948–954.
21. Steitz,T.A. (2005) On the structural basis of peptide-bond formation and antibiotic resistance from atomic structures of the large ribosomal subunit. *FEBS Lett*., **579**, 955–958.
22. Tucker,B.J. and Breaker,R.R. (2005) Riboswitches as versatile gene control elements. *Curr. Opin. Struct. Biol*., **15**, 342–348.
23. Mattick,J.S. and Makunin,I.V. (2005) Small regulatory RNAs in mammals. *Hum. Mol. Genet*., **14**, R121–132.
24. Matzke,M.A. and Birchler,J.A. (2005) RNAi-mediated pathways in the nucleus. *Nature Rev. Genet*., **6**, 24–35.
25. Willmann,M.R. and Poethig,R.S. (2005) Time to grow up: the temporal role of smallRNAs in plants. *Curr. Opin. Plant Biol*., **8**, 548–552.
26. Voinnet,O. (2005) Induction and suppression of RNA silencing: insights from viral infections. *Nature Rev. Genet*., **6**, 206–220.
27. Gottesman,S. (2005) Micros for microbes: non-coding regulatory RNAs in bacteria. *Trends Genet*., **21**, 399–404.
28. Westhof,E., Masquida,B. and Jaeger,L. (1996) RNA tectonics: towards RNA design. *Fold Des*., **1**, R78–R88.
29. Leontis,N.B. and Westhof,E. (2003) Analysis of RNA motifs. *Curr. Opin. Struct. Biol*., **13**, 300–308.
30. Cate,J.H., Yusupov,M.M., Yusupova,G.Z., Earnest,T.N. and Noller,H.F. (1999) X-ray crystal structures of 70S ribosome functional complexes. *Science*, **285**, 2095–2104.
31. Wimberly,B.T., Brodersen,D.E., Clemons,W.M.Jr, , Morgan-Warren,R.J., Carter,A.P., Vonrhein,C., Hartsch,T. and Ramakrishnan,V. (2000) Structure of the 30S ribosomal subunit. *Nature*, **407**, 327–339.
32. Ban,N., Nissen,P., Hansen,J., Moore,P.B. and Steitz,T.A. (2000) The complete atomic structure of the large ribosomal subunit at 2.4 A resolution. *Science*, **289**, 905–920.
33. Schluenzen,F., Tocilj,A., Zarivach,R., Harms,J., Gluehmann,M., Janell,D., Bashan,A., Bartels,H., Agmon,I., Franceschi,F. *et al*. (2000) Structure of functionally activated small ribosomal subunit at 3.3 angstroms resolution. *Cell*, **102**, 615–623.
34. Leontis,N.B., Stombaugh,J. and Westhof,E. (2002) The non-Watson–Crick base pairs and their associated isostericity matrices. *Nucleic Acids Res*., **30**, 3497–3531.
35. Jaeger,L., Westhof,E. and Leontis,N.B. (2001) TectoRNA: modular assembly units for the construction of RNA nano-objects. *Nucleic Acids Res*., **29**, 455–463.
36. Chworos,A., Severcan,I., Koyfman,A.Y., Weinkam,P., Oroudjev,E., Hansma,H.G. and Jaeger,L. (2004) Building programmable jigsaw puzzles with RNA. *Science*, **306**, 2068–2072.
37. Jaeger,L. and Leontis,N.B. (2000) Tecto-RNA: one-dimensional self-assembly through tertiary interactions. *Angew. Chem. Int. Ed*., **14**, 2521–2524.
38. Ikawa,Y., Fukada,K., Watanabe,S., Shiraishi,H. and Inoue,T. (2002) Design, construction, and analysis of a novel class of self-folding RNA. *Structure (Camb.)*, **10**, 527–534.
39. Horiya,S., Li,X., Kawai,G., Saito,R., Katoh,A., Kobayashi,K. and Harada,K. (2003) RNA LEGO: magnesium-dependent formation of specific RNA assemblies through kissing interactions. *Chem. Biol*., **10**, 645–654.
40. Ikawa,Y., Tsuda,K., Matsumura,S. and Inoue,T. (2004) De novo synthesis and development of an RNA enzyme. *Proc. Natl Acad. Sci. USA*, **101**, 13750–13755.
41. Liu,B., Baudrey,S., Jaeger,L. and Bazan,G.C. (2004) Characterization of tectoRNA assembly with cationic conjugated polymers. *J. Am. Chem. Soc*., **126**, 4076–4077.
42. Davis,J.H., Tonelli,M., Scott,L.G., Jaeger,L., Williamson,J.R. and Butcher,S.E. (2005) RNA helical packing in solution: NMR structure of a 30 kDa GAAA tetraloop-receptor complex. *J. Mol. Biol*., **351**, 371–382.
43. Hansma,H.G., Oroudjev,E., Baudrey,S. and Jaeger,L. (2003) TectoRNA and 'kissing-loop' RNA: atomic force microscopy of self-assembling RNA structures. *J. Microsc*., **212**, 273–279.
44. Shu,D., Moll,W.D., Deng,Z., Mao,C. and Guo,P. (2004) Bottom-up assembly of RNA arrays and superstructures as potential parts in nanotechnology. *Nano Lett*., **4**, 1717–1723.

45. Koyfman,A.Y., Braun,G., Magonov,S., Chworos,A., Reich,N.O. and Jaeger,L. (2005) Controlled spacing of cationic gold nanoparticles by nanocrown RNA. *J. Am. Chem. Soc*., **127**, 11886–11887.
46. Zuker,M. (2003) Mfold web server for nucleic acid folding and hybridization prediction. *Nucleic Acids Res*., **31**, 3406–3415.
47. Massire,C. and Westhof,E. (1999) MANIP: an interactive tool for modelling RNA. *J. Mol. Graph. Model*., **16**, 197–205, 255–257.
48. Rupert,P.B. and Ferre-D'Amare,A.R. (2001) Crystal structure of a hairpin ribozyme–inhibitor complex with implications for catalysis. *Nature*, **410**, 780–786.
49. Cate,J.H., Gooding,A.R., Podell,E., Zhou,K., Golden,B.L., Kundrot,C.E., Cech,T.R. and Doudna,J.A. (1996) Crystal structure of a group I ribozyme domain: principles of RNA packing [see comments]. *Science*, **273**, 1678–1685.
50. Walter,F., Murchie,A.I.H. and Lilley,D.M.J. (1998) Folding of the four-way RNA junction of the hairpin ribozyme. *Biochemistry*, **37**, 17629–17636.
51. Thomson,J.B. and Lilley,D.M. (1999) The influence of junction conformation on RNA cleavage by the hairpin ribozyme in its natural junction form. *RNA*, **5**, 180–187.
52. Klostermeier,D. and Millar,D.P. (2000) Helical junctions as determinants for RNA folding: origin of tertiary structure stability of the hairpin ribozyme. *Biochemistry*, **39**, 12970–12978.
53. Costa,M. and Michel,F. (1997) Rules for RNA recognition of GNRA tetraloops deduced by *in vitro* selection: comparison with *in vivo* evolution. *EMBO J*., **16**, 3289–3302.
54. Crane,H.R. (1950) Principles and problems of biological growth. *Sci. Mon*., **70**, 376–389.
55. Pauling,L. (1953) Protein interactions. Aggregation of globular proteins. *Discussions Faraday Soc*., **13**, 170–176.
56. Yeates,T.O. and Padilla,J.E. (2002) Designing supramolecular protein assemblies. *Curr. Opin. Struct. Biol*., **12**, 464–470.
57. Nogales,E. (2000) Structural insights into microtubule function. *Annu. Rev. Biochem*., **69**, 277–302.
58. Macnab,R.M. (2003) How bacteria assemble flagella. *Annu. Rev. Microbiol*., **57**, 77–100.
59. Goodsell,D.S. and Olson,A.J. (2000) Structural symmetry and protein function. *Annu. Rev. Biophys. Biomol. Struct*., **29**, 105–153.
60. Aguda,A.H., Burtnick,L.D. and Robinson,R.C. (2005) The state of the filament. *EMBO Rep*., **6**, 220–226.
61. Holmes,K.C., Popp,D., Gebhard,W. and Kabsch,W. (1990) Atomic model of the actin filament. *Nature*, **347**, 44–49.
62. Herrmann,H. and Aebi,U. (2004) Intermediate filaments: molecular structure, assembly mechanism, and integration into functionally distinct intracellular scaffolds. *Annu. Rev. Biochem*., **73**, 749–789.
63. Padilla,J.E., Colovos,C. and Yeates,T.O. (2001) Nanohedra: using symmetry to design self assembling protein cages, layers, crystals, and filaments. *Proc. Natl Acad. Sci. USA*, **98**, 2217–2221.
64. Ryadnov,M.G. and Woolfson,D.N. (2003) Engineering the morphology of a self-assembling protein fibre. *Nature Mater*., **2**, 329–332.
65. Guo,P.X., Erickson,S. and Anderson,D. (1987) A small viral RNA is required for *in vitro* packaging of bacteriophage phi 29 DNA. *Science*, **236**, 690–694.
66. Khaled,A., Guo,S., Feng,L. and Guo,P. (2005) Controllable self-assembly of nanoparticles for specific delivery of multiple therapeutic molecules to cancer cells using RNA nanotechnology. *Nano Lett*., **5**, 1797–1808.
67. Davidson,E.A. and Ellington,A.D. (2005) Engineering regulatory RNAs. *Trends Biotechnol*., **23**, 109–112.
68. Bates,A.D., Callen,B.P., Cooper,J.M., Cosstick,R., Geary,C., Glidle,A., Jaeger,L., Pearson,J.L., Proupín-Pérez,M., Xu,C. *et al.* (2006) Construction and characterization of a gold nanoparticle wire assembled using Mg2+-dependent RNA–RNA interactions. *Nano Lett*., in press.